The Monte Carlo Method: Versatility Unbounded In A Dynamic Computing World
Chattanooga, Tennessee, April 17–21, 2005, on CD-ROM, American Nuclear Society, LaGrange Park, IL (2005)

COMPREHENSIVE CROSS SECTION DATABASE DEVELOPMENT FOR GENERALIZED THREE DIMENSIONAL RADIATION TRANSPORT CODES: REPORT OF COMPLETION OF PHASE I

Thomas M. Miller and Lawrence W. Townsend
Department of Nuclear Engineering
The University of Tennessee
Pasqua Engineering Building
Knoxville, TN 37996
tmiller7@utk.edu; ltownsen@utk.edu

ABSTRACT

To correctly specify the composition and spectra of heavy ion radiation fields, such as those encountered in space radiation protection studies, as they are transported through shielding, accurate values of the total, elastic scattering, and reaction cross sections, spectral distributions and angular distributions of all emitted particles (nucleons, light ions and heavy ions) from the nuclear interactions of propagating high energy heavy ion (HZE) particles with target nuclei are required. For space radiation protection studies, this means that double-differential (energy and angle) isotope production cross sections must be known for all stable nuclear isotopes with mass numbers from 1 to about 60 colliding with any target nucleus at energies from tens of MeV per nucleon up to several GeV per nucleon. With this cross section database, transport codes would be able to transport nearly any radiation field that man or machine might be exposed to in space or otherwise. This database is the first high speed comprehensive database suitable for three dimensional radiation transport.

Key Words: Cosmic Rays, Monte Carlo, Nuclear Fragmentation, Charged Particle Transport

1 INTRODUCTION

For years NASA has investigated space radiation protection of astronauts and electronics. This research has included the creation of nuclear interaction models for the particles found in the space environment, transport codes that use these models to describe the changes in the space radiation fields as they penetrate shielding, and materials research to determine the best shield materials for these particles and even to create new shield materials for these particles. This research has traditionally differed from that done for terrestrial radiation protection because of the different particle species and energies of those particles present in their respective radiation environments. In recent years, as new higher power accelerator systems have been built and the interest in charged particle radiotherapy has grown, research on terrestrial and space radiation protection has converged. In spite of this convergence of interest the amount of research concerning radiations like those in the ambient space field increased only slightly. However, now that the United States has decided to return to the moon and to further explore Mars, interest in this research area has increased even more, and in turn, NASA is increasing the amount of research being carried out in this field. NASA realizes that for human exploration of Mars to be successful NASA's space radiation protection capabilities need to be improved. This research is

just one aspect of NASA's work that has sprouted from its new focus on space radiation protection.

2 EXSISTING DATABASES

Several algorithms necessary to transport particles using either stochastic or deterministic methods are already well known. What is needed to create a generalized three-dimensional radiation transport code is a comprehensive cross section database of total, elastic scattering, total reaction, and double differential particle production cross sections for virtually any colliding nuclear system.

Several cross section models currently exist that contain part of the information needed to construct a comprehensive cross section database for transport of high-energy heavy ions in three-dimensions. In their current states these cross section models are not designed to work together for a fully three-dimensional transport problem. The existing models of particular interest are:

- The heavy ion total and total reaction cross section databases for incident energies above 25 MeV/nucleon developed at NASA LaRC [1].
- The improved total reaction cross section database, above 1 MeV/nucleon developed at NASA LaRC [2].
- The nuclear fragmentation cross sections database for heavy ions developed at NASA LaRC [3].
- The total and total reaction cross section database for nucleon and deuteron interactions for incident energies above 25 MeV/nucleon developed at NASA LaRC [4].
- The nuclear fragmentation cross sections database for alpha particles developed at NASA LaRC [5].
- The microscopic model for the estimation of energy degradation in nucleus-nucleus collisions developed at the Naval Research Laboratory (NRL) [6].

2.1 Nuclear Fragmentation

The fragmentation of nuclei in this discussion is divided into two parts, first the fragmentation of nuclei with charge (Z) greater than 2 and second the fragmentation of nuclei with charge 1 and 2. These two divisions have been labeled heavy ions and light ions, respectively. The fragmentation of the heavy ions is handled by NUCFRG2 [3] and various other models handle the fragmentation of light ions. More information about how NUCFRG2 is used in this nucleus-nucleus event generator can be found in reference 7. Information about light ion fragmentation can be found in reference 8, but is updated here.

2.1.1 Light ion ($Z \leq 2$) fragmentation

The simplest projectile to determine the fragmentation products of is the deuteron because it only has one reaction channel:

$$^{2}H + X \rightarrow X + p + n\,. \quad (1)$$

Therefore, the total reaction cross section is equal to the production cross section of the deuteron's single reaction channel. Since the deuteron breakup cross section is equivalent to it total reaction cross section Tripathi's improved total reaction cross section [2] also serves as the deuteron breakup model.

Cucinotta, Townsend, and Wilson have developed a parameterization of helium-3, triton, and deuteron production due to alpha particle fragmentation on hydrogen targets. The cross section for helium-3 production is [5]:

$$\sigma_{He-3}^{Cucinotta} = 42.5\left[\frac{2}{1+e^{(T_{th}-T)/6.8}}-1\right]\left(1-\frac{0.51}{1+6.7e^{-T/34}}\right)^{3}\left[1+0.36\sqrt{\frac{T}{520}}\right]\left(e^{(780-T)/2300}\right), \quad (2)$$

where T_{th} is the threshold energy for the possible fragmentation events, which are listed below in Table I, and T is the kinetic energy of the projectile in units of MeV per nucleon [5].

Table I: Threshold Energies for Alpha-Hydrogen Fragmentation Channels [5]

Fragmentation Channel	Threshold, MeV
$^{4}He + p \rightarrow {}^{2}H + {}^{3}He$	22.94
$^{4}He + p \rightarrow p + p + {}^{3}H$	24.77
$^{4}He + p \rightarrow p + n + {}^{3}He$	25.72
$^{4}He + p \rightarrow p + {}^{2}H + {}^{2}H$	29.81
$^{4}He + p \rightarrow p + p + n + {}^{2}H$	32.59
$^{4}He + p \rightarrow p + p + p + n + n$	35.37

The cross section for triton production is [5]:

$$\sigma_{t}^{Cucinotta} = 15.5\left[\frac{2}{1+e^{(T_{th}-T)/7}}-1\right]\left(1-\frac{0.45}{1+7e^{-T/55}}\right)^{3}\left[1+1.8\sqrt{\frac{T}{550}}\right]\left(e^{(750-T)/4500}\right). \quad (3)$$

Lastly, the cross section for deuteron production is [5]:

$$\sigma_{d}^{Cucinotta} = 17\left[\frac{2}{1+e^{(T_{th}-T)/12}}-1\right]\left(1+\frac{\frac{0.21T}{145}-0.21}{1+e^{(145-T)/6}}\right)\left(e^{-T/3000}\right). \quad (4)$$

Another possible reaction channel is referred to as the pickup channel by Cucinotta, Townsend, and Wilson. This channel is essentially a coalescence channel and occurs when a neutron is removed from the alpha, which coalesces with the target proton. The cross section for the pickup channel is [5]:

$$\sigma_{pickup}^{Cucinotta} = 48e^{-(T-T_{th})^{1.7/1350}}\,. \quad (5)$$

In order to apply this model to any target, not just hydrogen targets, multiply $\sigma_{pickup}^{Cucinotta}$ by $A_T^{1/3}$, $\sigma_{He-3}^{Cucinotta}$ by $A_T^{0.31}$, $\sigma_t^{Cucinotta}$ by $A_T^{0.31}$, and $\sigma_d^{Cucinotta}$ by $A_T^{0.42}$.

Currently no models for helium-3 and triton fragmentation have been found in the open literature. However, in the code HZETRN [9] there exists an undocumented model for helium-3 and triton break up in the subroutine LIFRAG. This model seems very crude at first glance, but considering that there are only two possible fragmentation channels for each ion the actual fragmentation process itself is not very complex. The possible fragmentation channels for each ion are listed below in Table II.

Table II: Triton and Helium-3 Fragmentation Channels

Triton	Helium-3
$^3H + X \rightarrow X + p + n + n$	$^3He + X \rightarrow X + p + p + n$
$^3H + X \rightarrow X + n + {}^2H$	$^3He + X \rightarrow X + p + {}^2H$

The model states that the deuteron production cross section for tritons and helium-3 is 35 percent of the total reaction cross section [9]. Therefore, the triton fragmentation model is [9]:

$$\sigma_{nd} = 0.35 * \sigma_{reaction} \text{ and } \sigma_{pnn} = \sigma_{reaction} - \sigma_{nd}, \tag{6}$$

and the helium-3 fragmentation model is [8]:

$$\sigma_{pd} = 0.35 * \sigma_{reaction} \text{ and } \sigma_{ppn} = \sigma_{reaction} - \sigma_{pd}. \tag{7}$$

3 NUCLEUS-NUCLEUS EVENT GENERATOR

Now that the theories of several independent nuclear models have been discussed in Section 2 a discussion of how they will work together to form a nucleus-nucleus event generator is needed. Included in this discussion are some additional approximations and physics concepts that help to complete the picture that the nuclear models in Section 2 began to describe.

3.1 Total and Total Reaction Cross Sections

The total cross section is not calculated directly from the optical model developed by Townsend and collaborators [1,4]. The agreement of the total and total reaction cross sections as compared with experiment at energies around 2 GeV/nucleon is within about 3 percent [1]. For lower energies around 25 MeV/nucleon the agreement is on the order of 20 percent [1]. The error in the ratio of the total cross section to total reaction cross section is smaller than the error for the total cross section alone. Therefore, the ratio of the total cross section to total reaction cross section using the optical model is calculated using data that is given in references 1 and 4:

$$R = \frac{\sigma_{tot}^{optical}}{\sigma_R^{optical}}. \tag{8}$$

Then to actually calculate the total cross section, the total reaction cross section from Tripathi and collaborators' parameterization of total reaction cross sections [2] is multiplied by the ratio of the optical model total cross section to total reaction cross section:

$$\sigma_{tot} = R\sigma_R^{Tripathi}. \tag{9}$$

No significant errors are expected for ratios obtained by interpolating between the target mass numbers or projectile mass numbers of nuclei given in Townsend and collaborator's paper. Tripathi and collaborators' parameterization of total reaction cross sections is a more accurate model with smaller error at low energies than the total reaction cross section model developed by Townsend and collaborators. The total reaction cross section that was calculated from Tripathi and collaborators' parameterization, $\sigma_R^{Tripathi}$, will be reported as the total reaction cross section in this work.

As an example, the total and total reaction cross sections for ^{12}C colliding with ^{12}C is plotted in Figure 1 as a function of projectile kinetic energy. The total cross section in Figure 1 cuts off at 25 and 22500 MeV per nucleon because the referenced data cuts off at these energies. The total reaction cross section cuts off at 1 MeV per nucleon due to the restriction of the nuclear model. However, the total reaction cross section can be calculated above 22500 MeV per nucleon. Below 25 MeV per nucleon the event generator uses the cross section value at 25 MeV per nucleon, and does not allow any fragmentation below 25 MeV per nucleon. While this may be a poor approximation of the cross section ions below 25 MeV per nucleon have a very small range and do not travel far. Above 22500 MeV per nucleon the event generator uses the cross section value at 22500 MeV per nucleon. Cross sections above about 3000 MeV per nucleon are fairly constant, so this is a reasonable approximation.

3.2 Elastic Scattering Cross Section

The elastic scattering cross section is the difference between the total cross section and the total reaction cross section:

$$\sigma_{elastic} = \sigma_{tot} - \sigma_R^{Tripathi}. \tag{10}$$

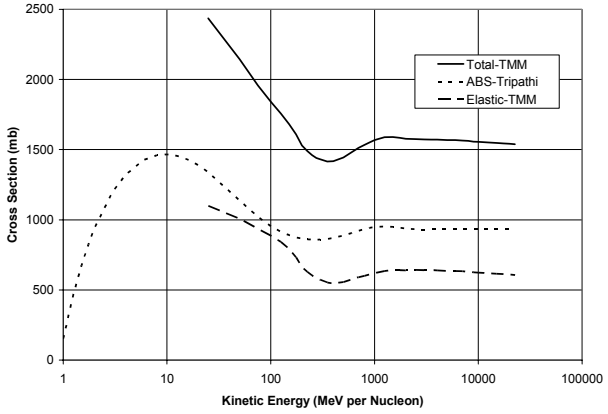

Figure 1: Total, Total Reaction, and Elastic Scattering Cross Sections for ^{12}C on ^{12}C

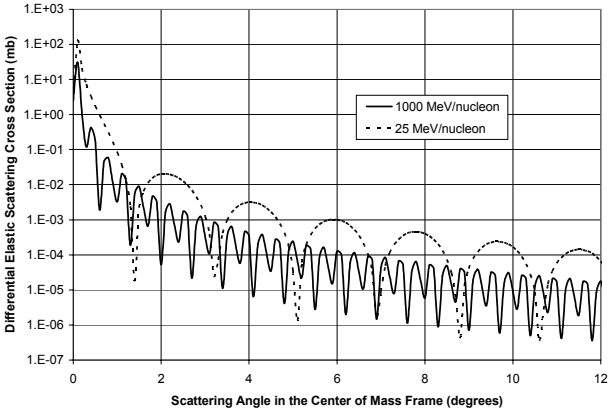

Figure 2: Differential Elastic Scattering Cross Section for ^{12}C on ^{12}C

Figure 1 also includes the elastic scattering cross section for ^{12}C on ^{12}C. In the event that an elastic scattering interaction occurs, particle kinematics is used to determine the new energy and direction of travel of the projectile and target [10]. This simply involves applying conservation of energy and momentum before and after the collision. To find the scattering angles of the projectile and target the Fraunhofer approximation, which is a semiclassical approach, is applied. It states that the scattering angle of the projectile in the center of mass frame is approximated by the following distribution [11]:

$$\frac{d\sigma}{d\Omega} = \left(kR_0^2\right)^2 \left(\frac{J_1\left(kR_0\theta\right)}{kR_0\theta} \right)^2 , \tag{11}$$

where θ is the scattering angle, R_0 is the radius of the target, k is the wave number of the projectile, and J_1 is the first order Bessel function of the first kind.

Figure 2 shows the differential elastic scattering cross section of ^{12}C on ^{12}C in the center of mass frame with projectile kinetic energies of 1000 and 25 MeV per nucleon as approximated by the Fraunhofer approximation. After the polar (z direction) scattering angle is chosen the remaining azimuthal scattering angles (between the x and y directions) for the target and projectile can be randomly sampled between 0-degrees and 360-degrees because elastic scattering is isotropic with respect to those angles.

3.3 Double Differential Fragmentation/Spallation Production Cross Sections

Unfortunately, there is no single nuclear model currently available that is capable of accurately predicting double differential cross sections for the production of all secondaries from nuclear collisions at all of the energies of interest within a reasonable period of time (hours to days). Neither is there sufficient experimental measurements of these double differential cross sections to use in database development for space radiation shielding and transport studies. Therefore, several nuclear models must be used in conjunction to predict double differential production cross sections for nucleus-nucleus collisions.

3.3.1 Heavy ion (Z > 2) production cross sections

NUCFRG2 accurately accounts for the yields of all light ion and heavy ion fragments produced by a nucleus-nucleus collision, with a projectile charge number greater than 2. However, in its original form the cross sections that NUCFRG2 provides are actually the probability of that fragment/spallation product being produced times the average multiplicity. In reality this is only a problem for the light ion products because the average multiplicity of the heavy ions in NUCFRG2 is one.

In order to clearly explain this problem with the average multiplicity let's consider the following reactions:

$$\begin{aligned} {}^{12}C + X &\rightarrow X' + {}^{11}B + p \\ {}^{12}C + X &\rightarrow X' + {}^{9}Be + d + p \end{aligned} , \tag{12}$$

where X is the target and X′ is all the target fragments. Assuming the first reaction listed above produces ^{11}B with a cross section of 10 mb, then the proton produced in that collision also has a production cross section of 10 mb. If the second reaction has a cross section for producing ^{9}Be

of 5 mb, then the deuteron and proton also have a 5 mb production cross section. In the end NUCFRG2 sums all the production cross sections for alphas, helium-3, tritons, deuterons, and protons and reports this sum for their respective production cross sections. So for our example in equation (22) ^{11}B has a cross section of 10 mb, ^{9}Be has a cross section of 5 mb, deuterons have a cross section of 5 mb, and protons have a cross section of 15 mb. For use in this nucleus-nucleus event generator, NUCFRG2 was modified. The modified version of NUCFRG2 is exactly the same as the original except the lines where these additional cross sections were added to the fragment cross section were commented out. Below Table III shows the production cross sections for ^{12}C on ^{12}C at 1 GeV per nucleon calculated by the original version of NUCFRG2 (labeled NF2) and the production cross sections for ^{12}C on ^{12}C at 1 GeV per nucleon calculated by the modified version of NUCFRG2 (labeled NF2-TMM).

One other correction that was necessary for NUCFRG2 dealt with neutron production. Looking at Table III one will notice that the neutron is not listed as a possible fragment. This is due to the fact that NUCFRG2 does not allow any neutron production in the fragmentation process, meaning that the remains of the fragment after ablation is never a neutron. Therefore, a rough estimate of the neutron production cross section, $\sigma_{neutron}$, can be attained by scaling the proton production cross section calculated by NUCFRG2, $\sigma_{proton\text{-}nf2}$:

$$\sigma_{neutron} = \frac{A_P - Z_P}{Z_P}\sigma_{proton}, \tag{23}$$

where A_p and Z_p are the mass and charge numbers of the projectile, respectively. Continuing the example started in Table III, neutron production cross section calculated using equation (23) would be 717.6099 mb.

3.3.2 Light ion ($Z \leq 2$) production cross sections

As was previously stated the deuteron breakup model is simply Tripathi's improved total reaction cross section model because there is only one possible reaction channel for a deuteron.

Table III: Production Cross Sections for ^{12}C on ^{12}C at 1 GeV per Nucleon with Average Multiplicities for Light Ions (mb)

Charge	Mass	NF2	NF2-TMM	Charge	Mass	NF2	NF2-TMM
6	11	52.9027	52.9027	3	10	2.52E-03	2.52E-03
6	10	0.353754	0.353754	3	9	3.42E-02	3.42E-02
6	9	2.73E-03	2.73E-03	3	8	0.106091	0.106091
6	8	2.30E-06	2.30E-06	3	7	20.5311	20.5311
5	11	53.11982	53.11982	3	6	28.61594	28.61594
5	10	54.56862	54.56862	2	9	4.61E-06	4.61E-06
5	9	3.07356	3.07356	2	8	3.35E-05	3.35E-05
5	8	1.60E-02	1.60E-02	2	6	0.36744	0.36744
5	6	3.75E-06	3.75E-06	**2**	**4**	**151.194**	**25.80074**
4	10	3.299027	3.299027	**2**	**3**	**11.72714**	**8.24591**
4	9	13.15494	13.15494	1	6	3.33E-05	3.33E-05
4	8	3.452457	3.452457	**1**	**3**	**23.45637**	**16.49329**
4	7	18.95178	18.95178	**1**	**2**	**61.88556**	**23.06178**
4	6	7.85E-02	7.85E-02	**1**	**1**	**4478.601**	**717.6099**

Figure 3 shows the deuteron on ^{12}C total reaction (or breakup) cross section as a function of projectile kinetic energy.

Cucinotta and collaborators' model for alpha fragmentation/spallation is used to determine the products of alpha-nucleus collisions. For alpha breakup the products of the reaction are determined by choosing the entire reaction channel of the alpha breakup. Figure 4 shows the fragmentation channel cross sections for an alpha on ^{12}C as a function of projectile kinetic energy. Figure 5 is the same as Figure 4 with the 2 proton 2 neutron channel removed to enable one to see the other channels more clearly.

Since there are only two fragmentation channels for both the triton and ^{3}He, the cross sections are used to pick the specific channels not just the individual fragments. Figure 6 shows the fragmentation channel cross sections for a triton on ^{12}C as a function of projectile kinetic energy, and Figure 7 shows the fragmentation channel cross sections for a ^{3}He ion on ^{12}C as a function of projectile kinetic energy.

3.3.3 Fragment kinetic energy and angular distributions

The microscopic model for the estimation of energy degradation in nucleus-nucleus collisions calculates the mean and standard deviation of fragment's kinetic energy distribution. Using the mean and standard deviation, a Gaussian distribution is sampled in order to pick a kinetic energy for the fragment. To illustrate, consider the interaction of ^{12}C at 1 GeV per nucleon with ^{12}C. Below in Table IV is an example a of possible fragmentation channel for this interaction. Listed for the fragmentation channel are the mean and standard deviation of each particle's kinetic energy distribution as given by Tsao and collaborators' model. The mean and standard deviation in Table IV are given in units of MeV per nucleon in the laboratory frame. This model assumes that light fragments are coincident with a heavier fragment, and that both have the same mean kinetic energy per nucleon. This assumption essentially says that all particles are treated as the fragment, i.e. the remains of the prefragment after ablation, when the mean kinetic energy is calculated by this model. However, this model is being applied not to only the fragment but also light ions that are evaporated from the prefragment and nucleons that are abraded from the projectile. Therefore, this assumption is only used in the nucleus-nucleus event generator for heavy fragments. When the mean and standard deviation of the kinetic energy distribution is being calculated for an evaporated particle or an abraded nucleon this assumption is not used. This allows for a broader range of kinetic energies to be realized, which is more consistent with experimental measurements of light ions and nucleons. To illustrate the difference, Table IV also shows the same particles resulting from the example interaction as, however, the model by Tsao and collaborators' has now been modified.

Finally, the angular distribution of particles produced in nucleus-nucleus interactions must be considered. This event generator does not use a specific nuclear model for selecting scattering angles during particle production. Instead it applies a few systematics of momentum distributions observed during experiments by Morrissey [12]. First, Morrissey stated that longitudinal momentum distributions of projectile-like particles are roughly isotropic in a rest frame moving with nearly the beam velocity. Therefore, the event generator samples scattering angles of particles emitted by the projectile isotropically in the projectile rest frame. Second, Morrissey stated that target-like particles' momentum distributions are essentially isotropic in a frame nearly at rest. Therefore, the event generator samples scattering angles of particles emitted by the target isotropically in the target rest frame, which is equivalent to the laboratory frame.

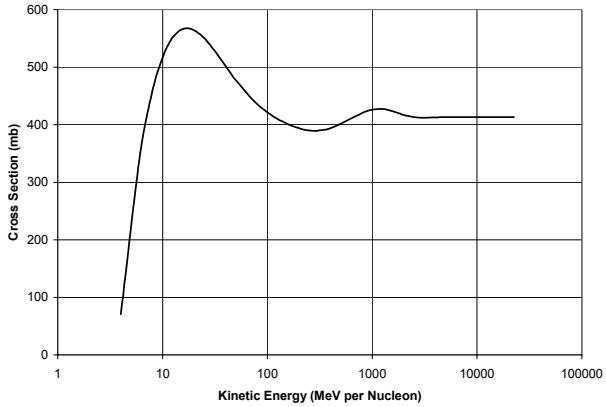

Figure 3: Deuteron on ^{12}C Total Reaction Cross Section

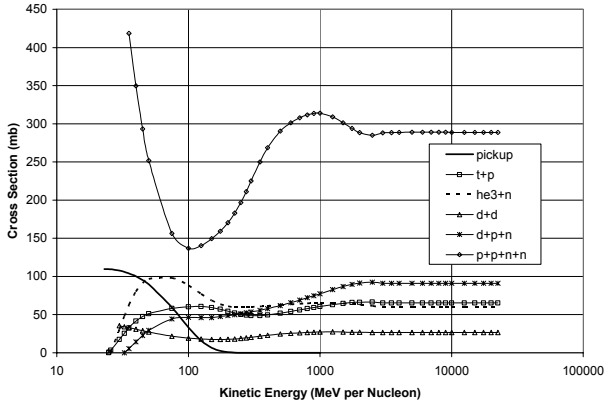

Figure 4: Alpha on ^{12}C Fragmentation Channel Cross Sections

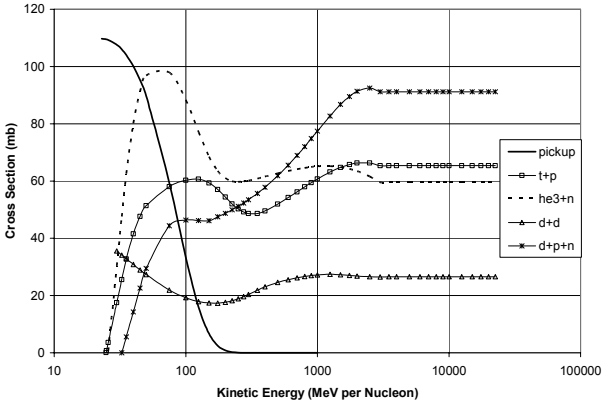

Figure 5: Alpha on ^{12}C Fragmentation Channel Cross Sections Excluding 2 p 2 n

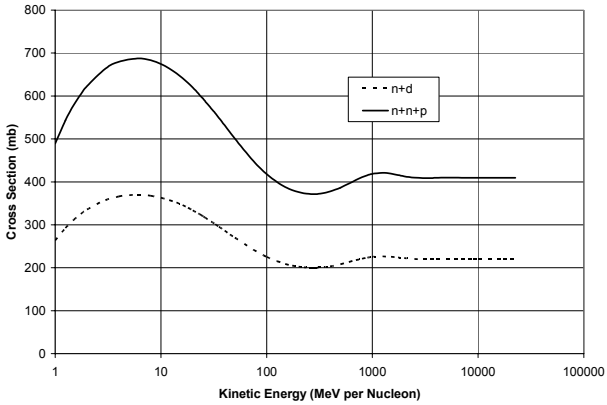

Figure 6: Triton on ^{12}C Fragmentation Channel Cross Sections

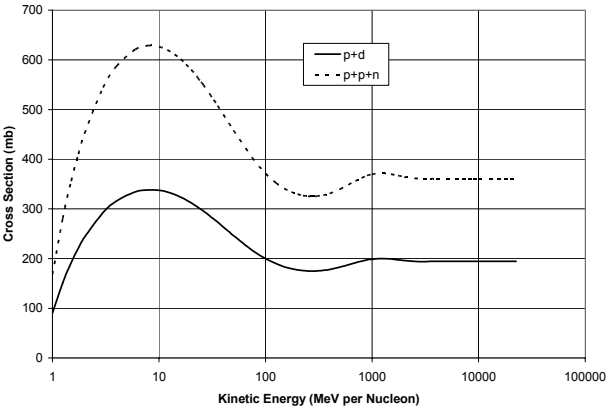

Figure 7: ^{3}He on ^{12}C Fragmentation Channel Cross Sections

Table IV: Example Means and Standard Deviations for Fragment Kinetic Energy Distributions of ^{12}C at 1 GeV per nucleon on ^{12}C

$^{12}C + {}^{12}C \rightarrow X + {}^{7}Li + {}^{3}He + p + n$							
Unmodified Model				**Modified Model**			
Charge	**Mass**	**Mean**	**Standard Deviation**	**Charge**	**Mass**	**Mean**	**Standard Deviation**
3*	7*	974.1	60.66	3*	7*	974.1	62.87
2	3	969.0	84.83	2	3	934.5	109.7
1	1	977.7	86.89	1	1	795.5	179.3
0	1	972.2	95.44	0	1	794.6	179.6
*Fragment, i.e. remains of prefragment after ablation (MeV per nucleon)							

3.4 Projectile and Target Role Reversal

To this point this discussion of the nucleus-nucleus event generator has centered on the projectile. That is because after the event generator chooses the projectile fragments and their energies and angles the role of projectile and target are reversed. Then with the actual target in the role of the projectile this same process is repeated to choose the target fragments and their energies and directions. The target, now in the role of the projectile, maintains the same kinetic energy per nucleon as the projectile. Essentially, the process of determining the results of target fragmentation is the same as determining the results of projectile fragmentation.

4 EVENT GENERATOR SAMPLE RESULTS

In order to better illustrate the capabilities of the newly created nucleus-nucleus event generator several calculations have been performed. These calculations were carried out to show that its results could be used to reproduce the inputs provided by the event generator's constituent models.

First the event generator was run to calculate the fragmentation production cross sections of ^{12}C at 1 GeV per nucleon on ^{12}C. This is an attempt to duplicate the results that were given by the modified version of NUCFRG2 previously listed in Table III. The event generator simulated ten million histories that resulted in inelastic collisions. The fragments (i.e., the remains of the prefragment) were counted and the production cross sections using the event generator were calculated. The production cross section for each fragment and the standard deviation of the mean for each fragment are reported in Table V. A few cross sections in Table V were calculated as zero. Two (^{10}Li and ^{9}He) are zero because even though NUCFRG2 calculates a cross section they physically are not possible because these ions have more neutrons than the projectile. The remaining ions with zero cross sections were not sampled in ten million histories.

Next, using the same example of ^{12}C at 1 GeV per nucleon on ^{12}C, the mean and standard deviation of each fragments' kinetic energy distribution for the reaction channel whose fragment (i.e. remains of the prefragment) is ^{7}Li, discussed in Table IV, were calculated. This is an attempt to reproduce the results of the modified model listed in Table IV. First, one million samples of the ^{7}Li kinetic energy distribution were collected in bins and plotted against the Gaussian function with the sample mean and standard deviation. These one million samples were taken independent of the other distributions, so conservation of energy was not required when taking these samples. This comparison is in Figure 8. Then one million samples of each fragments' kinetic energy distribution were taken, requiring energy to be conserved for each history. The resulting mean kinetic energies and standard deviations (of the sample, not the mean) for each

Table V: Event Generator Calculated Production Cross Sections for ^{12}C on ^{12}C at 1 GeV per Nucleon (mb) Compared to the Modified Version of NUCFRG2

Charge	Mass	NF2-TMM	Cross Section Calculated by Event Generator	Standard Deviation
6	11	52.9027	52.99084	0.095149
6	10	0.353754	0.353876	0.007894
6	9	2.73E-03	0.002818	0.000705
6	8	2.30E-06	0	
5	11	53.11982	53.15148	0.095288
5	10	54.56862	54.50833	0.096459
5	9	3.07356	3.086417	0.023296
5	8	1.60E-02	0.016558	0.001708
5	6	3.75E-06	0	
4	10	3.299027	3.297087	0.024077
4	9	13.15494	13.17514	0.047994
4	8	3.452457	3.420213	0.024521
4	7	18.95178	19.0015	0.057541
4	6	7.85E-02	0.070458	0.003523
3	10	2.52E-03	0	
3	9	3.42E-02	0.033291	0.002422
3	8	0.106091	0.107272	0.004347
3	7	20.5311	20.51141	0.059757
3	6	28.61594	28.7071	0.070528
2	9	4.61E-06	0	
2	8	3.35E-05	0.000176	0.000176
2	6	0.36744	0.382588	0.008208
2	4	25.80074	25.7151	0.066809
2	3	8.24591	8.215239	0.037952
1	6	3.33E-05	0	
1	3	16.49329	16.41445	0.05352
1	2	23.06178	23.01056	0.063248
1	1	717.6099	718.2144	0.273728
0	1	717.6099	717.0664	0.273659

fragment are shown in Table VI. The values in Table VI are in units of MeV per nucleon in the laboratory frame.

The final calculation done with the event generator looked at the momentum of the fragments produced by the reaction channel discussed in Table VI. This is an attempt to look at momentum conservation for projectile fragments in the projectile rest frame. The event generator assumes the projectile is traveling in the Z direction. The X, Y, and Z momentum components of fragments emitted from the projectile were summed over one million inelastic collisions of ^{12}C at 1 GeV per nucleon on ^{12}C. Then these sums for each collision were averaged and the standard deviation of the sample for each direction was calculated. The mean value and standard deviation of each momentum component's sum are shown in Table VII.

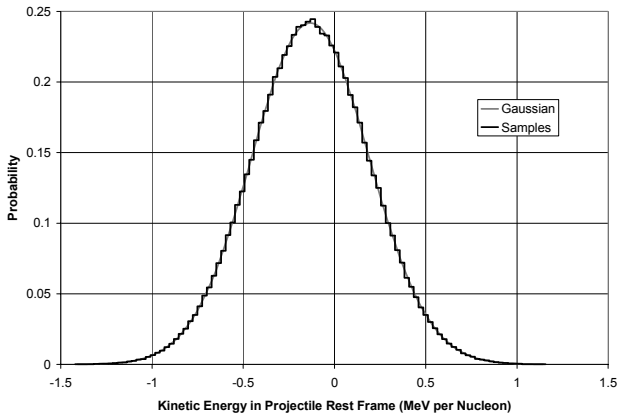

Figure 8: Fragment ^{7}Li Gaussian Kinetic Energy Distribution in the Projectile (^{12}C) Rest Frame

Table VI: Event Generator Calculated Means and Standard Deviations for Fragment Kinetic Energy Distributions of ^{12}C at 1 GeV per nucleon on ^{12}C

$^{12}C + {}^{12}C \rightarrow X + {}^{7}Li + {}^{3}He + p + n$					
Charge	**Mass**	**Mean**	**Standard Deviation**	**Event Generator Mean**	**Event Generator Stand. Dev.**
3*	7*	974.1	62.87	983.5	58.76
2	3	934.5	109.7	950.0	65.96
1	1	795.5	179.3	833.8	146.7
0	1	794.6	179.6	812.4	137.3
*Fragment, i.e. remains of prefragment after ablation (MeV per nucleon)					

Table VII: Event Generator Calculated Means and Standard Deviations for Sums of Projectile Fragments' Momentum Components (^{12}C at 1 GeV per nucleon on ^{12}C)

Momentum Component	**Mean of Resulting Momentum Component Sum**	**Standard Deviation of Resulting Momentum Components Sum**
X	-9.78E-02	30.96364
Y	4.06E-01	75.07322
Z	-95.3355	80.43794

5 CONCLUSIONS

The three calculations carried out with the event generator were intended to try and duplicate results of the constituent models that make up the event generator, and therefore show that the models are working as expected inside the event generator. The first calculation done with the event generator, whose results are in Table V, was an attempt to duplicate the results of the modified version of NUCFRG2 in Table III. Comparing the cross sections listed in Table V one sees that the event generator is producing each fragment isotope at the correct rate.

Next, an attempt was made to duplicate the results of the modified version of the microscopic model for the estimation of energy degradation in nucleus-nucleus collisions listed in Table IV. First, one million samples of the Gaussian kinetic energy distribution of ^{7}Li in the projectile rest frame were binned and plotted in Figure 8. Also in Figure 8 is the graph of a

Gaussian distribution with the same mean and standard deviation that was being used to sample the kinetic energy of ^{7}Li. Figure 8 clearly shows that the Gaussian is being sampled properly. However, it must be pointed out that these samples were taken independent of any other fragments, so conservation of energy was not considered in these samples. Table VI shows the average and standard deviation of the sample for one million samples of the kinetic energy distributions of the four fragments in the reaction channel being considered. These samples were all taken while considering conservation of energy. Comparing the results in Table VI to the model predictions one sees that the mean and standard deviation of the sample calculated by the event generator is different from what the kinetic energy degradation model calculated. This difference is due to conservation of energy being implemented with a rejection method. This is also due to the fact that the kinetic energy degradation model calculates the mean and standard deviation for each fragment's Gaussian kinetic energy distribution without considering any of the other fragments. Due to this rejection method samples will inevitably be thrown out and samples in the tails of the kinetic energy distributions may become even less likely to be chosen. It should be pointed out that the energies eventually chosen by this rejection method are a subset of the possible energies predicted by the kinetic energy degradation model. This can been seen in Table VIII, which shows the mean plus and minus 3.29 standard deviations (99.9% confidence interval) for the kinetic energy degradation model and the event generator predictions.

The final calculation performed with the event generator considered the selection of scattering angles for projectile fragments and conservation of momentum in the projectile rest frame. It was stated earlier that projectile fragments are isotropically distributed in the projectile rest frame by the event generator. This is an approximation to the observation made by Morrissey that projectile like fragments are isotropically distributed in a frame moving nearly with the same velocity as the projectile. This implies that the net momentum components of fragments in the X, Y, and Z directions on the average should sum to zero. This would certainly be the case in the frame that the fragments are truly isotropically distributed in. However, in the projectile rest frame this is not exactly true. The reason for this goes back to the sampling of kinetic energies. On the average fragments in the projectile rest frame have been downshifted in kinetic energy, i.e. their velocity is slower than that of the projectile. Therefore, on the average, more fragments in the projectile rest frame have momentum vectors that point in the negative Z direction (assuming the projectile was traveling parallel to the positive Z axis). This is illustrated in Table VII where the average sum of momentum components in the X and Y directions is close to zero, but the average sum of the Z momentum component is less than zero.

Table VIII: Domain of 99.9 Percent of Kinetic Energy Samples for the Kinetic Energy Degradation Model and the Event Generator

		Kinetic Energy Degradation Model Domain		Event Generator Domain	
Charge	**Mass**	**$\mu - 3.29\sigma$**	**$\mu + 3.29\sigma$**	**$\mu - 3.29\sigma$**	**$\mu + 3.29\sigma$**
3*	7*	767.3	1180.9	790.2	1176.8
2	3	573.6	1295.4	733.0	1167.0
1	1	205.6	1385.4	351.2	1316.4
0	1	203.7	1385.5	360.7	1264.1
*Remains of prefragment after ablation (MeV per nucleon)					

6 ACKNOWLEDGMENTS

The authors gratefully acknowledge the NASA Graduate Student Research Program (GSRP) fellowship from NASA's Marshall Space Flight Center for financial support. Research support from NASA under grant no. NAG 8-1669 is also gratefully acknowledged.

7 REFERENCES

1. L. W. Townsend, J. W. Wilson, and H. B. Bidasaria, "Heavy-Ion Total and Absorption Cross Sections above 25 MeV/Nucleon," *NASA Technical Paper No. TP-2138* (1983).
2. R. K. Tripathi, F. A. Cucinotta, and J. W. Wilson, "Universal Parameterization of Absorption Cross Section: Light Systems," *NASA Technical Paper No. TP-209726* (1999).
3. J. W. Wilson, J. L. Shinn, L. W. Townsend, R. K. Tripathi, F. F. Badavi and S. Y. Chun, "NUCFRG2: A Semiempirical Nuclear Fragmentation Model," *Nuclear Instruments and Methods in Physics Research, Part B*, **94**, p. 95 (1994).
4. L. W. Townsend, J. W. Wilson, and H. B. Bidasaria, "Nucleon and Deuteron Scattering Cross Sections From 25 MeV/Nucleon to 22.5 GeV/Nucleon," *NASA Technical Memorandum No. TM-84636* (1983).
5. F. A. Cucinotta, L. W. Townsend, and J. W. Wilson, "Description of Alpha-Nucleus Interaction Cross Sections for Cosmic Ray Shielding Studies," *NASA Technical Paper No. TP-3285* (1993).
6. C. H. Tsao, R. Silberberg, A. F. Barghouty, and L. Shiver, "Energy Degradation in Cosmic-Ray Nuclear Spallation Reactions: Relaxing the Straight-Ahead Approximation," *The Astrophysical Journal*, **451**, p. 275 (1995).
7. T. M. Miller and L.W. Townsend, "Double-Differential Heavy-Ion Production Cross Sections," *Radiation Protection Dosimetry*, **110**, p. 53 (2004)
8. T. M. Miller and L.W. Townsend, "Double-Differential Light-Ion Production Cross Sections," *Radiation Protection Dosimetry*, **110**, p. 57 (2004)
9. J. W. Wilson, F. F. Badavi, F. A. Cucinotta, J. L. Shinn, G. D. Badhwar, R. Silberberg, C. H. Tsao, L. W. Townsend, and R. K. Tripathi, "HZETRN: Description of a Free-Space Ion and Nucleon Transport and Shielding Computer Program" *NASA Technical Paper 3495* (1995).
10. E. Byckling and K. Kajantie, *Particle Kinematics*, John Wiley & Sons, London (1973).
11. H. Fraunfelder and E. M. Henley, *Subatomic Physics*, Prentice Hall Inc., Englewood Cliffs, NJ (1974).
12. D. J. Morrissey, "Systematics of Momentum Distributions from Reactions with Relativistic Ions," *Physical Review, Part C*, **39**, p. 460 (1989).